



香港城市大學
City University of Hong Kong

專業 創新 胸懷全球
Professional · Creative
For The World

CityU Scholars

Modeling and Analysis for Modulation of Light-Conversion Materials in Visible Light Communication

Xiao, Xiangtian; Xiao, Hua; Liu, Haochen; Wang, Rui; Choy, Wallace C. H.; Wang, Kai

Published in:
IEEE Photonics Journal

Published: 01/10/2019

Document Version:
Final Published version, also known as Publisher's PDF, Publisher's Final version or Version of Record

License:
CC BY

Publication record in CityU Scholars:
[Go to record](#)

Published version (DOI):
[10.1109/JPHOT.2019.2931611](https://doi.org/10.1109/JPHOT.2019.2931611)

Publication details:
Xiao, X., Xiao, H., Liu, H., Wang, R., Choy, W. C. H., & Wang, K. (2019). Modeling and Analysis for Modulation of Light-Conversion Materials in Visible Light Communication. *IEEE Photonics Journal*, 11(5), [8201113].
<https://doi.org/10.1109/JPHOT.2019.2931611>

Citing this paper

Please note that where the full-text provided on CityU Scholars is the Post-print version (also known as Accepted Author Manuscript, Peer-reviewed or Author Final version), it may differ from the Final Published version. When citing, ensure that you check and use the publisher's definitive version for pagination and other details.

General rights

Copyright for the publications made accessible via the CityU Scholars portal is retained by the author(s) and/or other copyright owners and it is a condition of accessing these publications that users recognise and abide by the legal requirements associated with these rights. Users may not further distribute the material or use it for any profit-making activity or commercial gain.

Publisher permission

Permission for previously published items are in accordance with publisher's copyright policies sourced from the SHERPA RoMEO database. Links to full text versions (either Published or Post-print) are only available if corresponding publishers allow open access.

Take down policy

Contact lbscholars@cityu.edu.hk if you believe that this document breaches copyright and provide us with details. We will remove access to the work immediately and investigate your claim.

Modeling and Analysis for Modulation of Light-Conversion Materials in Visible Light Communication

Volume 11, Number 5, October 2019

Xiangtian Xiao

Hua Xiao

Haochen Liu

Rui Wang

Wallace C. H. Choy, *Senior Member, IEEE*

Kai Wang, *Member, IEEE*



Glass Container with green QDs solution



Glass Container with red QDs solution

DOI: 10.1109/JPHOT.2019.2931611

Modeling and Analysis for Modulation of Light-Conversion Materials in Visible Light Communication

Xiangtian Xiao,^{1,2,*} Hua Xiao^{1,3,*} ,^{3,*} Haochen Liu,¹ Rui Wang,¹
Wallace C. H. Choy,² *Senior Member, IEEE*,
and Kai Wang¹ , *Member, IEEE*

¹Academy for Advanced Interdisciplinary Studies, Department of Electrical and Electronic Engineering, Southern University of Science and Technology, Shenzhen, Guangdong 518055, China

²Department of Electrical and Electronic Engineering, The University of Hong Kong, Hong Kong

³Department of Electronic Engineering, City University of Hong Kong, Kowloon, Hong Kong

DOI:10.1109/JPHOT.2019.2931611

This work is licensed under a Creative Commons Attribution 4.0 License. For more information, see <https://creativecommons.org/licenses/by/4.0/>

Manuscript received June 13, 2019; revised July 14, 2019; accepted July 24, 2019. Date of publication July 29, 2019; date of current version September 30, 2019. This work was supported in part by National Natural Science Foundation of China under Grant 61875082, in part by Natural Science Foundation of Guangdong (2017B030306010), in part by Shenzhen Innovation Project (JCYJ20160301113537474), and in part by Shenzhen Key Laboratory for Advanced Quantum Dot Displays and Lighting (ZDSYS201707281632549). (Xiangtian Xiao^{*} and Hua Xiao^{*} contributed equally to this work.) Corresponding authors: Wallace C. H. Choy and Kai Wang (e-mail: chchoy@eee.hku.hk and wangk@sustc.edu.cn).

Abstract: Visible light communication (VLC) is a kind of high-efficiency wireless communication technology. As one of the key issues in VLC, the modulation bandwidth of light-conversion materials based light-emitting diodes (LEDs) has gained considerable attention in recent years. However, few people focus on theoretical analyses of the light-conversion process during modulation, which show significant influence on the modulation bandwidth of a white LED. In this work, we proposed low-pass filter based models of light-conversion materials of YAG:Ce phosphor and CdSe/ZnS quantum dots, to build the relationship between fluorescence lifetime of these light-conversion materials and their modulation bandwidth. Furthermore, the modulation bandwidth of light source with polychromatic light was obtained and analyzed based on the proposed model. The experimental results of the modulation bandwidth showed a highly consistency with the results from simulation models. These analyses were believed to help realizing white-light illumination with high bandwidth. To the best of our knowledge, this is the first time the modulation mechanisms of light-conversion materials in VLC have been comprehensively discussed in literature.

Index Terms: Light-emitting diodes, Optical materials, Optical communication.

1. Introduction

As an efficient wireless communication technology, visible light communication (VLC) has gained considerable attention nowadays [1]–[6]. By modulating high frequency visible light, illumination and optical communication can be realized simultaneously. Owing to advantages of high rate in transmission, excellent performance in security, and low energy consumption, VLC systems are potentially to be applied as facilities in for accommodation, medical treatment, and automotive lighting [7], [8].

Conventionally, phosphors are adopted to produce white light in VLC because of their low cost, wavelength tunability, and matured technology. However, many commercial phosphors can only produce narrow modulation bandwidth with approximately 1 MHz due to their long fluorescence lifetime [9], [10]. Since the bandwidth of a light source shows significant influence on communication rate, the application of phosphor based LEDs is gradually limited [11]. To improve the bandwidth of the light source, researchers try different methods to produce optimized light-conversion materials with short fluorescence lifetime. Xiao [12] *et al.* and Ruan [13] *et al.* reported the implementation of CdSe/ZnS and AgInS₂/ZnS quantum dots (QDs) for light conversion in high power LEDs. These two types of QDs improve the bandwidth to 2.7 MHz (with fluorescence lifetime of 26.3 ns) and 5.4 MHz (with fluorescence lifetime of 77.0 ns), respectively. Sajjad [14] *et al.* proposed to use oligofluorene-boron dipyrromethene (BODIPY) as the red conversion material for LEDs in VLC system. This organic semiconductor provides a short fluorescence lifetime of approximately 4 ns with bandwidth of 39 MHz. Additionally, Sajjad [15] *et al.* proposed green BBEHP-PPV and orange-red emitting MEH-PPV, which can offer fluorescence lifetime of 0.3 ns and bandwidth of 200 MHz. Dursun [16] *et al.* reported the application of CsPbBr₃ perovskite nanocrystals film as light-conversion materials, with bandwidth of 491.4 MHz and fluorescence lifetime of 7 ns. Y. Zhang [17] *et al.* proposed to use aggregation induced emission luminogens (AIEgens) in VLC, with 6-dB electrical modulation bandwidth up to 279 MHz. These methods received considerable attention, owing to the significant improvement in material performance. However, most of them focus on the bandwidth improvement by using different light-conversion materials, few of them analyzed and explained related mechanisms. Since these mechanisms directly determine the communication performance of material based devices, they become key issues in VLC.

To investigate the modulation performance of light-conversion materials, researchers such as H. Cao [18] and D. Xue [19] use an equation to describe the frequency-response of the color converter, however, without further explanation and derivation on the equation. In another word, recent relating references still lack of detailed information on the origination and mechanism of modulation characteristics of light-conversion materials.

In this study, mathematical models were built to connect bandwidth and properties of light-conversion materials. First, we built the a low-pass filter model for light-conversion materials, explaining the relationship between fluorescence lifetime and bandwidth. Then, frequency response curves were experimentally obtained to check the correctness of this model. Furthermore, the bandwidth of light source with polychromatic light was analyzed with the proposed model. These analyses were believed to help understanding diverse light-conversion processes in LED modulation, and realizing high bandwidth communication with high-end white-light illumination in the future. To the best of our knowledge, this is the first time the modulation mechanisms of light-conversion materials have been comprehensively discussed in literature.

To verify the accuracy of these models, related experiments were implemented. We designed a bandwidth measuring system for light-conversion materials by using direct current power supply, signal generator, bias-tee, photodetector (PD), and digital oscilloscope. Then, different types of light-conversion materials, including green, red, and yellow Y₃Al₅O₁₂:Ce³⁺ (YAG:Ce) phosphors, as well as green and red CdSe/ZnS QDs, were measured and analyzed. We compared (a) the obtained frequency response and bandwidth results with (b) the low-pass filter model based theoretical prediction results. Results showed that our model successfully described the influence of the fluorescence lifetime on the bandwidth, and proved the coincidence between simulation results and experimental data. Our work deduced the mathematical expression of frequency response and revealed the modulation mechanisms for light-conversion materials, providing methods to further optimize the bandwidth of light source in VLC.

2. Model and Discussion

In previous research, the modulation bandwidth of polychromatic light was usually obtained by measurement, without related theoretical analyses. Here, we built a modulation model for light

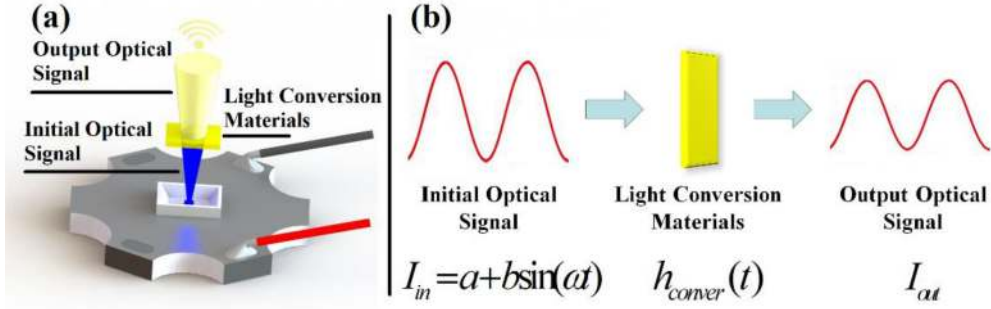


Fig. 1. (a) Light source structure; (b) transmission process of optical signal.

sources to understand the basic principle of optical signals in transmission, and the impact of light-conversion materials on the frequency response of the VLC system.

2.1 Basic Modulation Model for Light Conversion Materials

The basic modulation model for light-conversion materials is demonstrated based on the derivation of the fundamental knowledge in reference [20]. As shown in Fig. 1(a), the emitted blue light pass through the yellow light-conversion material, and completely converted into yellow light as a sine wave. As shown in Fig. 1(b), the output optical signal can be described as:

$$I_{out}(t) = I_{in}(t) * h_{conver}(t) = \int_0^{\infty} I_{in}(\tau) h_{conver}(t - \tau) d\tau, \quad (1)$$

where $I_{in}(t)$ is the light intensity of initial optical signal, $h_{conver}(t)$ is the impulse response of the light-conversion material. For bandwidth measuring, we use coupled signal with direct current (DC) and alternating current (AC, in shape of sine wave) to describe the input signal as follows

$$I_{in} = a + b \sin \omega t, \quad (2)$$

where a is the corresponding light intensity to the bias voltage, and b is the corresponding light intensity to the sine wave amplitude. Since light-conversion materials can be regarded as Linear Time-invariant (LTI) system, its impulse response can be described by a fitting curve of first-order fluorescence lifetime:

$$h_{conver}(t) = I(t) = I_0 \exp(-t/\tau), \quad (3)$$

where τ is the average fluorescence lifetime of light conversion materials, I_0 is the maximum fluorescence intensity. Thus, $I_{out}(t)$ can be deduced as follows.

$$\begin{aligned} I_{out}(t) &= \int_0^{\infty} h_{conver}(t') I_{in}(t - t') dt' \\ I_{out}(t) &= I_0 \int_0^{\infty} \exp(-t'/\tau) [a + b \sin(\omega t - \omega t')] dt' \\ I_{out}(t) &= I_0 \int_0^{\infty} [a \exp(-t'/\tau) + I_0 \int_0^{\infty} b \exp(-t'/\tau) \sin(\omega t - \omega t')] dt' \\ I_{out}(t) &= I_0 \left[a + b \int_0^{\infty} \exp(-t'/\tau) \sin(\omega t - \omega t') dt' \right] \\ I_{out}(t) &= I_0 \left[a + b \sin \omega t \int_0^{\infty} (\exp(-t'/\tau) \cos \omega t') dt' - b \cos \omega t \int_0^{\infty} (\exp(-t'/\tau) \sin \omega t') dt' \right] \end{aligned}$$

$$I_{out}(t) = I_0 \left[a + b \left(\frac{\omega\tau^2}{1 + \omega^2\tau^2} \sin \omega t - \frac{\tau}{1 + \omega^2\tau^2} \cos \omega t \right) \right]$$

$$I_{out}(t) = I_0 \left[a + \frac{b\tau}{\sqrt{1 + \omega^2\tau^2}} \left(\frac{\omega\tau}{\sqrt{1 + \omega^2\tau^2}} \sin \omega t - \frac{1}{\sqrt{1 + \omega^2\tau^2}} \cos \omega t \right) \right]$$

The final expression of light intensity of the output signal is described as:

$$I(t) = I_0 \left[a + \frac{b\tau}{\sqrt{1 + \omega^2\tau^2}} \sin(\omega t - \phi) \right], \quad (4)$$

where ϕ is the phase angle, and $\cos \phi$ can be expressed as:

$$\cos \phi = \frac{\omega\tau}{\sqrt{1 + \omega^2\tau^2}}. \quad (5)$$

Here we obtain the light intensity $I_{out}(t)$ by receiving signal from the PD. According to [12], in the operating range, the photovoltage of PD increases proportionally to light intensity of the AC signal component. Therefore, the amplitude of transfer function $|G_s|$ can be obtained when we only consider the alternating current signal component:

$$|G_s| = |U_{out}/U_{in}| = \left| \frac{\frac{I_0 b \tau}{\sqrt{1 + \omega^2 \tau^2}} \sin(\omega t - \phi)}{I_0 b \tau \sin(\omega t)} \right| = \frac{1}{\sqrt{1 + \omega^2 \tau^2}} \quad (6)$$

where U_{out} is the output voltage and U_{in} is input voltage. Therefore, the frequency response can be expressed by

$$R_{fre} = 10 \lg \left(\left(\frac{U_{out}}{U_{in}} \right)^2 \right) = 10 \lg \left(\frac{1}{1 + \omega^2 \tau^2} \right) = 10 \lg \left(\frac{1}{1 + (2\pi f)^2 \tau^2} \right). \quad (7)$$

Furthermore, when $R_{fre} = 10 \lg(\frac{1}{2}) \approx -3$ in Eq. (7), the corresponding frequency f is defined as the 3-dB modulation bandwidth (f_{3-dB}). Here,

$$f_{3-dB} = \frac{1}{2\pi\tau}. \quad (8)$$

Eq. (8) shows that the 3-dB modulation bandwidth of light-conversion materials is tightly depends on its fluorescence lifetime (τ). Thus, the bandwidth expression of light-conversion materials is proved successfully. Especially, LED chips also has the same form as follows:

$$f_{chip-3dB} = \frac{1}{2\pi\tau_{chip}}, \quad (9)$$

where the 3-dB modulation bandwidth of LED chips is relied on the efficient lifetime of carriers' recombination (τ_{chip}):

2.2 Modulation Model for Polychromatic Light

In Section 2.1, we assume that the initial light is completely converted by the light-conversion material. However, in VLC system, polychromatic light is usually used as a light source to realize optical communication. Thus, we illustrate the light-conversion process of LED based polychromatic light. As shown in Fig. 2, the initial light from the chip are incompletely converted, in which the residual incident light is mixing with the converted light in polychromatic light.

In this section, sine-wave from the chip is also used as initial optical signal for modulation, similar to that in Section A. Based on our analyses of Eq. 4 in Section A, the light intensity of polychromatic

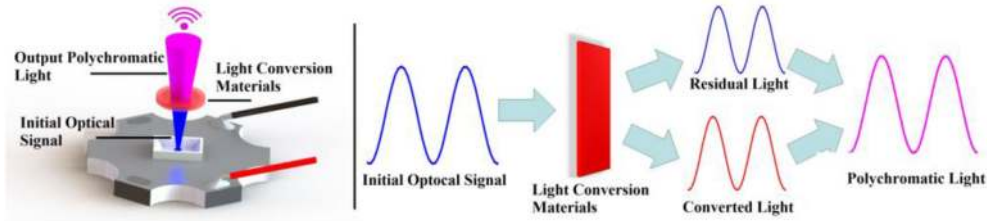


Fig. 2. (a) light source structure; (b) transmission process of polychromatic light.

light (I_{poly}) can be expressed as follows.

$$\begin{aligned} I_{poly} &= I_{residual} + I_{converted} \\ &= R_{residual} \cdot I_{in} + \frac{R_{converted}}{\sqrt{1 + (2\pi f)^2 \tau^2}} I_{in}(\phi), \end{aligned} \quad (10)$$

where $I_{residual}$ and $I_{converted}$ are the light intensity of residual light and converted light. $R_{residual}$ is the ratio of intensity amplitude of residual light signal and initial light signal. $R_{converted}$ is the ratio of intensity amplitude of converted light signal and initial light signal, where

$$R_{residual} = \frac{I_{res}}{I_{in}} = \frac{\Phi_{res}}{\Phi_{in}}, \quad (11)$$

$$R_{converted} = \frac{I_{conver}}{I_{in}} = \frac{\Phi_{conver}}{\Phi_{in}}. \quad (12)$$

Φ_{res} , Φ_{conver} and Φ_{in} are luminous flux of residual light, converted light, and initial light, respectively. These parameters can be measured by applying voltage on LED that equivalent to a + b. a and b are defined by Eq. (2) already. Besides, here we assume that the signal acceptance angle is small enough, so light intensity is uniform in the detection zone of the detector. The optical power of LED can be described as:

$$P_{\lambda_i} = \frac{I_{\lambda_i} \Omega}{V_{\lambda_i}}, \quad (13)$$

where P_{λ_i} is the optical power, V_{λ_i} is the standard normalized CIE photopic spectral luminous efficiency function, Ω is solid angle. When we modulate the frequency, Eq. (10) can be expressed in form of optical power as follows.

$$P_{poly} = R_{residual} \cdot P_{in} + \frac{R_{converted}}{\sqrt{1 + (2\pi f)^2 \tau^2}} P_{in}(\phi). \quad (14)$$

Since the residual signal and converted signal in Eq. (14) can be rewritten as two cosine signals, the optical power amplitude (A_{poly}) can be obtained based on cosine law:

$$A_{poly} = \sqrt{R_{residual}^2 + \frac{1}{1 + (2\pi f)^2 \tau^2} R_{converted}^2 + \frac{2R_{converted}R_{residual} \cos \Delta\phi}{1 + (2\pi f)^2 \tau^2}}, \quad (15)$$

where $\Delta\phi$ is the phase difference between converted light and residual light. Since residual light and initial light have the same phase, $\Delta\phi$ also is the phase difference between converted light and initial light, which can be calculated by Eq. (5). In addition, in Eq. (4), we use sine function to describe the signal, but here we use cosine function to calculate the value of A_{poly} , which leads to a phase difference of $\pi/2$. Therefore, based on formula 5, the following relation can be obtained as:

$$\cos\left(\frac{\pi}{2} - \phi\right) = \frac{\omega\tau}{\sqrt{1 + \omega^2\tau^2}}, \quad (16)$$

where $\omega = 2\pi f$. In our model, the magnitude of modulation frequency is MHz (10^6 Hz), and the magnitude of τ is ns (10^{-9} s). So $\omega\tau$ is very small (≈ 0). In this case, $\cos(\frac{\pi}{2} - \phi) \approx 0$, and $\cos \phi \approx 1$. As a result, the optical power amplitude (A_{poly}) can be obtained as follows:

$$A_{poly} = \sqrt{R_{residual}^2 + \frac{R_{converted}^2 + 2R_{converted}R_{residual}}{1 + (2\pi f)^2\tau^2}}. \quad (17)$$

In addition, it should be noticed that Eq. (17) is used for polychromatic light including two light (residual light and converted light). For white light that includes three parts (red, green, and blue, RGB light), the total optical power amplitude A_1 of two light (e.g., R + G) should be calculated first as follows:

$$A_1 = \sqrt{A_{red}^2 + A_{green}^2 + 2A_{red}A_{green} \cos \phi_1}, \quad (18)$$

where A_{red} and A_{green} is the optical power amplitude of red and green light, $\cos \phi_1$ is the phase difference between red and green light, which can be proved to be 1 by Eq. (16). Then the optical power A_{white} of white light can be obtained based on optical power amplitude of blue light and A_1 as follows:

$$A_{white} = \sqrt{A_1^2 + A_{blue}^2 + 2A_1A_{blue} \cos \phi_2}, \quad (19)$$

where $\cos \phi_2$ is the phase difference between red and green light, which can be proved as 1 (similar to $\cos \phi_1$). Therefore, this model can also be applied to white light.

Furthermore, the relationship between optical power $P_{optical}^2$ and electric power $P_{electric}$ can be described as:

$$P_{electric} \propto i^2 \propto P_{optical}^2, \quad (20)$$

where i is the current produced by PD.

Therefore, the frequency response of polychromatic light can be calculated as:

$$R_{poly} = 10 \lg \left(\left(\frac{P_{electric}(f)}{P_{electric}(0)} \right) \right) = 10 \lg \left(\left(\frac{A_{poly}^2(f)}{A_{poly}^2(0)} \right) \right), \quad (21)$$

According to the definition of A_{poly} in Eq. (17), R_{poly} can be shifted as follows:

$$R_{poly} = 10 \lg \left[\left(R_{residual}^2 + \frac{R_{converted}^2 + 2R_{converted}R_{residual}}{1 + (2\pi f)^2\tau^2} \right) / \left(R_{residual}^2 + R_{converted}^2 + 2R_{converted}R_{residual} \right) \right], \quad (22)$$

Through proper simplification, the frequency response of polychromatic light can be expressed by:

$$R_{poly} = 10 \lg \left(\frac{R_{residual}^2 + \frac{R_{converted}^2 + 2R_{converted}R_{residual}}{1 + (2\pi f)^2\tau^2}}{R_{residual}^2 + R_{converted}^2 + 2R_{converted}R_{residual}} \right). \quad (23)$$

According to Eq. (23), if the light is completely converted ($R_{residual} = 0$), the frequency response of polychromatic light can be rewritten as Eq. (7). If no light is converted, the frequency response will equal to zero, and optical power amplitude will not change with different modulation frequency. It is important to mention that if the light is partly converted, the frequency response will depend on the fluorescence lifetime of light-conversion materials and the proportion of converted and residual light in polychromatic light. According to Eq. (10), the increase in the proportion of converted light will cause increasing decay rate of frequency response and the 3-dB modulation bandwidth, if the response of the light-conversion material is slow (e.g. commercial yellow phosphors). Furthermore, based on Eq. (11) and Eq. (12), numerous characteristics of the materials, including thickness, concentration, area, and light-conversion efficiency, will have influence on the key parameters of

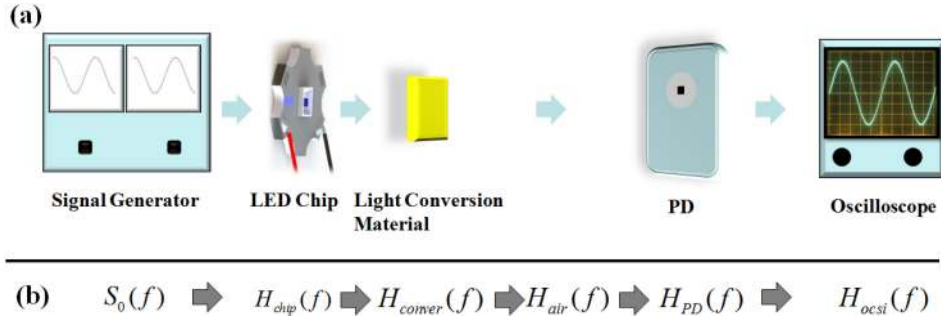


Fig. 3. Schematic of modulation bandwidth measuring. (a) Measuring system of our samples. (b) The illustration of frequency response of this system.

$R_{residual}$ and $R_{converted}$, thereby producing numerous influences on frequency response and modulation bandwidth. Also, we should notice that the proportion of converted light will affect the color and color temperature of polychromatic light. Therefore, balancing the modulation bandwidth and lighting quality is a potential issue for light source optimizing in VLC system.

Additionally, we let $R_{poly} = 10 \lg(1/2)$ in Eq. (23), the 3-dB modulation bandwidth of polychromatic light can be obtained as follows.

$$f_{3\text{-dB}} = \left[\frac{R_{converted}^2 + 2R_{converted}R_{residual} + R_{residual}^2}{R_{converted}^2 + 2R_{converted}R_{residual} - R_{residual}^2} \cdot \frac{1}{(2\pi\tau)^2} \right]^{\frac{1}{2}}. \quad (24)$$

Here we assume that the 3-dB bandwidth of initial light signal is infinite. Therefore, $\frac{R_{converted}}{(R_{converted} + R_{residual})} > 0.5$ must be satisfied for the calculation of 3-dB bandwidth, otherwise the 3-dB bandwidth will be infinity. On the other hand, for light sources (e.g., LED chips) in practical use, their 3-dB bandwidth cannot be infinite. We set the 3-dB bandwidth of the light source as B_{source} , the modulation model for this system can be described as: (a) a signal with infinite 3-dB bandwidth is transferred to optical signal by light source with 3-dB bandwidth B_{source} , (b) this optical signal pass through light-conversion materials, and (c) divided to converted light and residual light. In this case, once $R_{residual} \geq R_{converted}$, 3-dB bandwidth of this system will be higher than that of light conversion materials. When $R_{residual} \ll R_{converted}$, 3-dB bandwidth of this system is near to B_{source} .

2.3 Transmission Model

Fig. 3 shows the basic schematic of modulation bandwidth measurement. Firstly, the signal generator produces an electrical signal in sine wave. Then, this signal is converted to optical signal by the LED chip. While transmission in light-conversion materials and air, this optical signal is converted to electrical signal again by PD, and finally received by oscilloscope. Based on these transmission processes, the received signal can be expressed by:

$$S_r(f) = S_0(f) \cdot H_{chip}(f) \cdot H_{conver}(f) \cdot H_{air}(f) \cdot H_{PD}(f) \cdot H_{ocsi}(f), \quad (25)$$

where $S_r(f)$ is the received signal of sine wave, $S_0(f)$ is the initial signal of sine wave, $H_{chip}(f)$, $H_{conver}(f)$, $H_{air}(f)$, $H_{PD}(f)$ and $H_{ocsi}(f)$ are the frequency response of LED chip, light-conversion materials, air, PD, and oscilloscope, respectively. Since modulation bandwidth of air and oscilloscope are wide enough in this measuring system, $H_{air}(f)$ and $H_{ocsi}(f)$ can be ignored. Meanwhile, the expression of $H_{chip}(f)$ and $H_{PD}(f)$ has already been described in [20], [21]. Therefore, Eq. (25) can be rewritten in frequency domain as follows.

$$S_r(f) = S_0(f) \cdot H_{chip}(f) \cdot H_{conver}(f) \cdot H_{PD}(f), \quad (26)$$



Fig. 4. Modulation bandwidth measuring system.

where $H_{chip}(f) = 1/\sqrt{(1 + 2\pi f^2)\tau_{chip}^2}$, $H_{PD}(f) = 1/\sqrt{(1 + 2\pi f^2)\tau_{PD}^2}$, τ_{chip} is the efficient lifetime of carriers' recombination, τ_{PD} is the spent time of falling edge in PD response curve. The frequency response of light-conversion materials ($H_{conver}(f)$) of completely and partly converted light can be obtained according to Eq. (7) and Eq. (23), respectively.

Eq. (25) can accurately explain all the influences in VLC bandwidth measurement. Based on this result, we can easily conclude that we need to know $H_{chip}(f)$ and $H_{PD}(f)$ before we obtain the exact bandwidth of light-conversion materials. Therefore, $\tau_{chip}(f)$ and $\tau_{PD}(f)$ should be far shorter than fluorescence lifetime of light-conversion materials. When the modulation bandwidth of LED chip is too small (e.g., commercial high-power LED chip), it will affect bandwidth measurement for light conversion materials. Therefore, micro-LED and laser diode (LD) with more than 100 MHz 3-dB modulation bandwidth have been applied to ensure the system performance, as reported in [22]–[24]. On the other hand, the converted proportion of light is also an important parameter for the modulation bandwidth of incompletely converted light. Especially, the modulation bandwidth of the light source should be higher than that of the light-conversion materials, so that the modulation bandwidth will not become a limitation for the bandwidth measurement of light-conversion materials.

3. Experiments and Verification of Results

3.1 Measurement System and Materials Preparation

As shown in Fig. 4, we use a modulation bandwidth measuring system with a 0.5 W commercial blue LED chip (size 2835), direct current (DC) stabilized power supply, a signal generator (KEYSIGHT S1180A, 500 MHz), a DC-coupled Si transimpedance amplified photodetector (THORLABS PDA10A) with bandwidth of 150 MHz, and an oscilloscope (KEYSIGHT MSOX6004A, 1 GHz). When we turn on the LED, the signal generator simultaneously produce a output by coupling sinusoidal-wave signal and DC bias voltage. When light of biased LED is converted by phosphors or QDs, the emitting polychromatic light is mixed with modulated signal generated by LED and light-conversion materials, respectively. By adjusting the frequency of the signal generator, we can observe a shifting trend of sinusoidal signal on the oscilloscope. Through this process, we can easily measure the frequency response and 3-dB modulation bandwidth of LED.

For samples of light-conversion materials, we prepared yellow, green, and red YAG:Ce phosphors, as well as green and red CdSe/ZnS QDs with different concentrations, as shown in Fig. 5. Since phosphors were in solid state, we made phosphor-silicone slices by mixing silicone and phosphors in vacuum environment. To realize QD slice, we package QDs solution into specially-designed glass containers, which have the same dimension as that of phosphors.

3.2 Measurement for Completely Converted Light

For the measurement of intrinsic bandwidth for light-conversion materials, we use the color filter to prevent residual blue light and obtain completely converted light. The 3-dB modulation bandwidth of LED chip and PD were measured to be 7.9 MHz and 50 MHz. Therefore, $S_r(f)$ can be

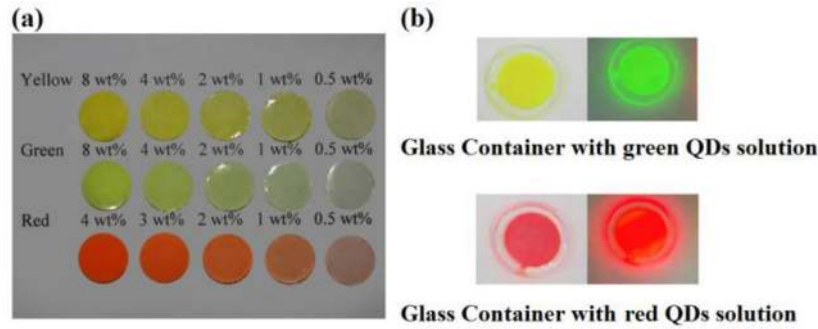


Fig. 5. Fabrication of (a) yellow, green and red phosphor layers with different concentration, and (b) green and red QD layers under ambient and UV environment.

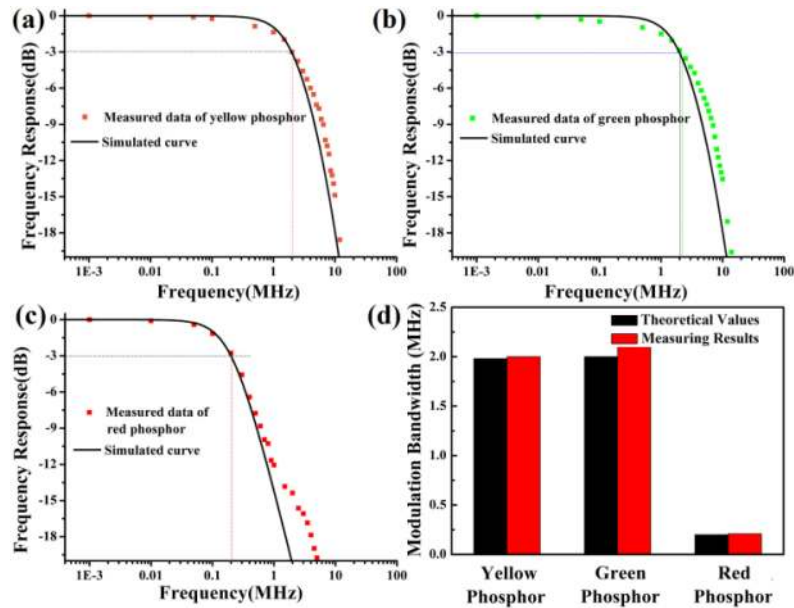


Fig. 6. Measured and simulated frequency responses of (a) yellow phosphor, (b) green phosphor, (c) red phosphor. (d) The comparison between 3-dB modulation bandwidth of theoretical and measured results.

expressed as:

$$S_r(f) = S_0(f) \cdot \frac{1}{\sqrt{1 + (f/7.9)^2}} \cdot \frac{1}{\sqrt{1 + (2\pi f)^2 \tau^2}} \cdot \frac{1}{\sqrt{1 + (f/50)^2}}, \quad (27)$$

where the fluorescence lifetime τ of yellow, green, and red phosphor was 59.80 ns, 55.00 ns, and 700.00 ns, respectively. For QDs, the fluorescence lifetime τ of green and red QDs were 22.00 ns and 26.10 ns.

Fig. 6(a), (b), and (c) show the measured and simulated frequency responses for yellow, green, and red phosphors. We can clearly observe the similar decreasing tendency between the simulated and experimental curves. Especially, the simulated curve can accurately describe the frequency response around 3-dB modulation bandwidth. As shown in Fig. 6(d), the simulated and measured bandwidth of yellow, green, and red phosphors are 1.98 MHz and 2.00 MHz; 2.00 MHz and 2.12 MHz; 0.2 MHz and 0.21 MHz, respectively. Based on the aforementioned results, our simulation

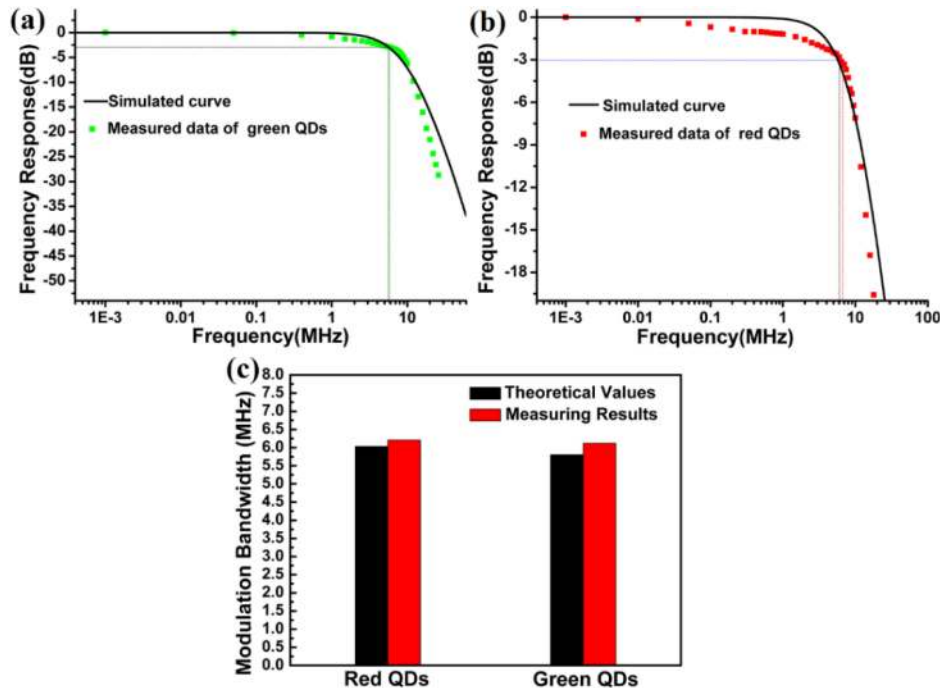


Fig. 7. Measured and simulated frequency responses for (a) green QDs, (b) red QDs. (c) The comparison between 3-dB modulation bandwidth of theoretical and measured results of red and green QDs.

and experiment results in frequency response and 3-dB modulation bandwidth are match well for completely converted light.

Additionally, for red phosphor, when the modulated frequency is far higher than 3-dB modulation bandwidth, the difference between simulated and measured curves becomes increasingly apparent. This is because the bandwidth of red phosphor is extremely low. When the frequency is increasing, system noise and low signal-noise ratio are unavoidable.

Fig. 7(a) and (b) show the measured and simulated frequency responses for green and red QDs. The simulated and measured curves have similar decrease tendency when the frequency is less than 10 MHz. Once this value is higher than 10 MHz, a small difference appears between measured and simulated response. As expected, the simulated curve can accurately describe the frequency response around 3-dB modulation bandwidth. As shown in Fig. 7(c), the simulated and measured bandwidth for green and blue QDs are 6.03 MHz and 6.21 MHz, 5.80 MHz and 6.12 MHz, respectively.

3.3 Measurement for Partly Converted Polychromatic Light

Based on Eq. (23), variation in proportion of converted light will alter the frequency response, and thereby affect the value of 3-dB modulation bandwidth of the LED. Hence, related parameters can be tuned to observe the variation tendency of 3-dB modulation bandwidth.

As shown in Fig. 8, thickness and concentration of light-conversion materials are modulated to observe the shifting in 3-dB modulation bandwidth. With the same thickness, higher concentration leads to lower bandwidth. Similarly, with the same concentration, higher thickness leads to lower bandwidth of the LED. These results are reasonable and coincident with expectation according to the bandwidth calculation in Eq. (24). Higher concentration and greater thickness will lead to higher light intensity of converted light, increasing the optical power of converted light. In another word, $R_{converted}$ is higher, and $R_{residual}$ is lower. According Eq. (24), the increase in the proportion

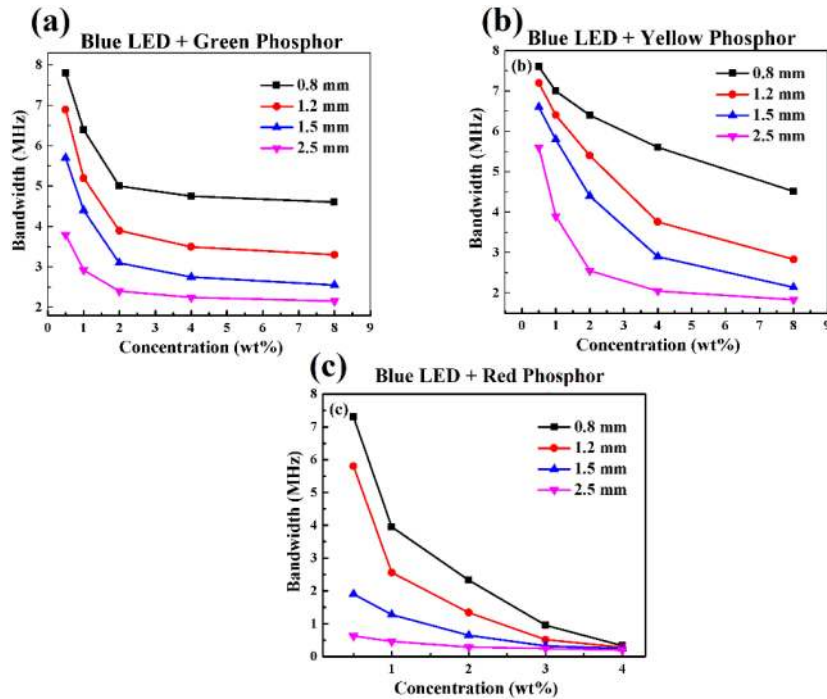


Fig. 8. Bandwidth of LED with phosphor and QD slides with different concentration and thickness.

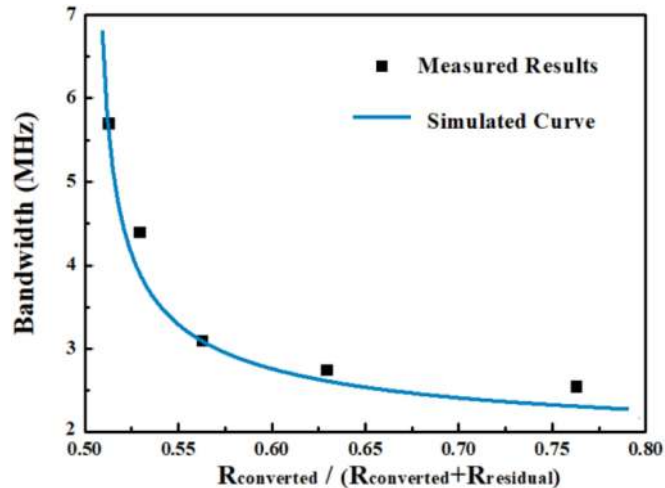


Fig. 9. Simulated and measured bandwidth for the blue LED chip covered by green phosphors with different $R_{converted} / (R_{converted} + R_{residual})$.

of converted light leads to rapid decline of frequency response. Therefore, the total bandwidth becomes lower.

Finally, the 3-dB bandwidth of polychromatic light is quantitatively studied by simulation. Here, we chose the green-phosphor as the target sample. Based on Eq. (24), the measured and simulated bandwidth results for converted light of green phosphors is compared and shown in Fig. 9. We did not use color filter, so emitted polychromatic light includes two parts: converted green light and residual blue light. According to Eq. (24), the increase in the proportion of converted light ($R_{converted}$)

leads to the decline of bandwidth. As shown in Fig. 9, the simulated curve is well match with the experimental results, indicating that our method can accurately describe the 3-dB modulation bandwidth. In Fig. 9, x axis starts from 0.5. This is because the relationship $\frac{R_{\text{converted}}}{(R_{\text{converted}}+R_{\text{residual}})} \geq 0.5$ is required to reach 3-dB bandwidth according to the definition of bandwidth. Additionally, x axis stops at 1, where light is completely converted. In another word, when $\frac{R_{\text{converted}}}{(R_{\text{converted}}+R_{\text{residual}})} = 1$, the final result will become the bandwidth of phosphor. Thus,

$$f_{3\text{-dB}} = \frac{1}{2\pi\tau} \approx 2 \text{ MHz.} \quad (28)$$

Also there are some little differences between simulated and measured curves. System noise and low signal-noise ratio may contribute to this phenomenon.

4. Conclusion

In this work, we built modulation models of light-conversion materials for VLC. First, a low-pass filter model of light-conversion materials were built to demonstrate the key relationship between fluorescence lifetime and bandwidth. Then, the bandwidth of light source with polychromatic light was analyzed based on the proposed model. Furthermore, we mathematically built a modulation bandwidth measuring system to obtain the frequency response of different light-conversion materials. The transmission model was also analyzed to ensure the accuracy of modulation bandwidth measurement. The experimental results show a highly consistency between proposed models and measured frequency responses. These analyses were believed to help realizing high bandwidth communication and white-light illumination simultaneously.

References

- [1] L. Wang, C. Wang, X. Chi, L. Zhao, and X. Dong, "Optimizing SNR for indoor visible light communication via selecting communicating LEDs," *Opt. Commun.*, vol. 387, pp. 174–181, 2017.
- [2] N. Chi, M. Zhang, Y. Zhou, and J. Zhao, "3.375-Gb/s RGB-LED based WDM visible light communication system employing PAM-8 modulation with phase shifted Manchester coding," *Opt. Exp.*, vol. 24, no. 19, pp. 21663–21673, 2016.
- [3] H. Li, X. Chen, J. Guo, and H. Chen, "A 550 mbit/s real-time visible light communication system based on phosphorescent white light led for practical high-speed low-complexity application," *Opt. Exp.*, vol. 22, no. 22, pp. 27203–13, 2014.
- [4] H. Chun *et al.*, "LED based wavelength division multiplexed 10 Gb/s visible light communications," *J. Lightw. Technol.*, vol. 34, no. 13, pp. 3047–3052, Jul. 2016.
- [5] P. Adasme, "Visible light communication networks under ring and tree topology constraints," *Comput. Stand Interface*, vol. 52, pp. 10–24, 2017.
- [6] Y. Q. Wang, Y. G. Wang, N. Chi, J. J. Yu, and H. L. Shang, "Demonstration of 575-Mb/s downlink and 225-Mb/s uplink bi-directional SCM-WDM visible light communication using RGB LED and phosphor-based LED," *Opt. Exp.*, vol. 21, no. 1, pp. 1203–1208, 2013.
- [7] H. Elgala, R. Mesleh, and H. Haas, "Indoor optical wireless communication: Potential and state-of-the-art," *IEEE Commun. Mag.*, vol. 49, no. 9, pp. 56–62, Sep. 2011.
- [8] L. Grobe *et al.*, "High-speed visible light communication systems," *IEEE Commun. Mag.*, vol. 51, no. 12, pp. 60–66, Dec. 2013.
- [9] H. Li *et al.*, "682 Mbit/s phosphorescent white LED visible light communications utilizing analog equalized 16QAM-OFDM modulation without blue filter," *Opt. Commun.*, vol. 354, pp. 107–111, 2015.
- [10] C. H. Yeh, Y. L. Liu, and C. W. Chow, "Real-time white-light phosphor-LED visible light communication (VLC) with compact size," *Opt. Exp.*, vol. 21, no. 22, pp. 26192–26197, 2013.
- [11] G. Ren, S. He, and Y. Yang, "Improving bandwidth efficiency of indoor visible light communication by M-ary return-to-zero optical pulse amplitude modulation," *J. Inf. Technol.*, vol. 12, no. 5, pp. 975–982, 2013.
- [12] X. T. Xiao *et al.*, "Improving the modulation bandwidth of LED by CdSe/ZnS quantum dots for visible light communication," *Opt. Exp.*, vol. 24, no. 19, pp. 21577–2158, 2016.
- [13] C. Ruan *et al.*, "White light-emitting diodes based on AgInS₂/ZnS quantum dots with improved bandwidth in visible light communication," *Nanomaterials*, vol. 6, no. 1, 2016, Art. no. 13.
- [14] M. T. Sajjad *et al.*, "Fluorescent red-emitting BODIPY Oligofluorene star-shaped molecules as a color converter material for visible light communications," *Adv. Opt. Mater.*, vol. 3, no. 4, pp. 536–540, 2015.
- [15] M. T. Sajjad *et al.*, "A novel fast color-converter for visible light communication using a blend of conjugated polymers," *ACS Photon.*, vol. 2, no. 2, pp. 194–199, 2015.

- [16] I. Dursun *et al.*, "Perovskite nanocrystals as a color converter for visible light communication," *ACS Photon.*, vol. 3, no. 7, pp. 1150–1156, 2016.
- [17] Y. Zhang *et al.*, "Aggregation-induced emission luminogens as color converters for visible-light communication," *ACS Appl. Mater. Interfaces*, vol. 10, pp. 34418–34426, 2018.
- [18] H. Cao, S. Lin, Z. Ma, X. Li, J. Li, and L. Zhao, "Color converted white light-emitting diodes with 637.6 MHz modulation bandwidth," *IEEE Elect. Device Lett.*, vol. 40, no. 2, pp. 267–270, Feb. 2019.
- [19] D. Xue *et al.*, "Enhanced bandwidth of white light communication using nanomaterial phosphors," *Nanotechnology*, vol. 29, no. 45, pp. 1–16, 2018.
- [20] J. R. Lakowicz, *Principles of Fluorescence Spectroscopy*. New York, NY, USA: Springer, 2006, Ch. 5.
- [21] T. P. Lee and A. G. Dentai, "Power and modulation bandwidth of GaAs-AlGaAs high-radiance LED's for optical communication systems," *IEEE J. Quantum Elect.*, vol. 14, no. 3, pp. 150–159, Mar. 1978.
- [22] C. H. Zheng, J. Chen, C. Yu, and M. Gurusamy, "Inverse design of LED arrangement for visible light communication systems," *Opt. Commun.*, vol. 382, no. 1, pp. 615–623, 2017.
- [23] R. X. G. Ferreira *et al.*, "High bandwidth GaN-based micro-LEDs for multi-Gb/s visible light communications," *IEEE Photon. Technol. Lett.*, vol. 28, no. 19, pp. 2023–2026, Oct. 2016.
- [24] J. R. D. Retamal *et al.*, "4-Gbit/s visible light communication link based on 16-QAM OFDM transmission over remote phosphor-film converted white light by using blue laser diode," *Opt. Exp.*, vol. 23, no. 26, pp. 33656–33666, 2015.